Coastal Engineering 169 (2021) 103972

Contents lists available at ScienceDirect

Coastal Engineering

journal homepage: www.elsevier.com/locate/coastaleng

Particle capture by seagrass canopies under an oscillatory flow

Aina Barcelona [a,*], Carolyn Oldham [b], Jordi Colomer [a], Jordi Garcia-Orellana [c,d], Teresa Serra [a]

[a] Department of Physics, University of Girona, 17071, Girona, Spain
[b] School of Engineering, The University of Western Australia, Perth, WA, 6009, Australia
[c] Departament of Física, Universitat Autònoma de Barcelona (UAB), Campus UAB, 08193, Bellaterra, Barcelona, Spain
[d] Institut de Ciència i Tecnologia Ambientals, Z Building, Universitat Autònoma de Barcelona (UAB), Campus UAB, 08193, Bellaterra, Barcelona, Spain

ARTICLE INFO

Keywords:
Seagrass
Sediment transport
Oscillatory flow
Turbulent kinetic energy
Sediment capture
Sedimentation

ABSTRACT

Although seagrass canopies are known to enhance particle sedimentation, there is still limited knowledge about how seagrasses modify the vertical distribution of sediment particles; especially when particles come from allochthonous sources. This study determined the volume of particles trapped by the seagrass leaves, the amount that remains in suspension both within and above the canopy, and the amount deposited onto the seabed. A set of laboratory experiments were conducted in which hydrodynamic conditions and canopy densities were varied to mimic real field conditions. This study demonstrated and quantified previously recorded observations concerning the fate of sediment in seagrass meadows. Seagrass meadows decreased the amount of suspended sediment by capturing the sediment on the blades of the seagrass and by enhancing particle sedimentation on the seabed. However, particles trapped by the blades of seagrass in the whole canopy increased with canopy density and reduced the number of particles in suspension within the canopy. The ecological implications were significant, since a seabed covered by vegetation, when compared to a bare seabed, produced a reduction in the suspended sediment particles within the canopy, improving water clarity. Furthermore, canopies (compared to bare substrates) enhanced seabed sedimentation and the denser the canopy was, the greater the amount of sediment deposited on the seabed.

1. Introduction

Seagrass canopies formed by *Posidonia oceanica* (Linnaeus) Delile or *Cymodocea nodosa* (Ucria) Ascherson are recognized in the EU Water Framework Directive (Community, 2000) as water quality indicators as they provide many ecosystem functions and services and maintain the complex structure of habitats (Brodersen et al., 2017b; Zucchetta et al., 2016). Species diversity in seagrasses increases with the structural complexity of the seagrass canopies (González-Ortiz et al., 2016). Seagrass meadows also play a role in 'blue carbon' sequestration because suspended particulate organic carbon can be trapped and buried by canopy action, thus mitigating the effect of the ongoing increase in CO_2 (Armitage and Fourqurean, 2016; Ricart et al., 2017). Furthermore, because damage to or the destruction of seagrass meadows can cause a release of carbon to the environment (Fourqurean et al., 2012), in developing 'blue carbon' strategies, management authorities and stakeholders could restore carbon sequestration capacities through coastal restoration projects (Duarte et al., 2013, 2015).

Allochthonous sediment particles transported by currents can impact coastal seagrass meadows negatively and consequently reduce the services they provide (Fraser et al., 2017). Some natural origins of the allochthonous sediment input can be coastal runoff, river plumes or natural resuspension (Pineda et al., 2016). Climate change has led to an increase in the frequency and intensity of heavy precipitation episodes which, in turn, has increased episodic river and runoff outflow (Vautard et al., 2014). Coastal development is also responsible for moving large amounts of sediment that can impact seagrass meadows (Wu et al., 2017). Suspended sediment input increases turbidity in the water column (Pineda et al., 2016; Wu et al., 2017; Roy et al., 2013), leading to a decrease in light intensity that then limits phytoplankton and seagrass growth, and buries benthic communities (Fraser et al., 2017; Vanderploeg et al., 2007; Longstaff and DennisonW.C., 1999).

Seagrass beds are one of the most valuable habitats in coastal zones because they promote the reduction of suspended particles within the seagrass meadows. Seagrasses affect particle sediment fluxes by reducing flow velocity, increasing sediment deposition and, via the plant

* Corresponding author.
E-mail addresses: aina.barcelona@udg.edu (A. Barcelona), carolyn.oldham@uwa.edu.au (C. Oldham), jordi.colomer@udg.edu (J. Colomer), jordi.garcia@uab.cat (J. Garcia-Orellana), teresa.serra@udg.edu (T. Serra).

https://doi.org/10.1016/j.coastaleng.2021.103972
Received 15 July 2020; Received in revised form 10 June 2021; Accepted 4 August 2021
Available online 4 August 2021

leaves themselves within the seagrass canopy capturing particles (Granata et al., 2001; Hendriks et al., 2008), decreasing sediment resuspension (Gacia et al., 1999; Zong and Nepf, 2011). Hence, the allochthonous suspended sediment that is advected over a canopy can remain in suspension in the water column inside the canopy, or settle to the seabed and possibly be resuspended, or be captured by the seagrass. That said, little information is available about the physical role the canopy densities play in trapping particles and thus improving carbon sequestration in coastal waters (Greiner et al., 2016; Marbà et al., 2015). Until now, the effect seagrasses have on the fate of particles from allochthonous sources in coastal areas has been studied observationally. For instance, Lawson et al. (2012) found an increase in the sediment suspended from the seabed in low densities of *Agarophyton vermiculophylla* (Ohmi) Gurgel, although J.N Norris & Fredericq compared this with higher densities. Through field observations, Gacia et al. (1999) determined that, when compared to bare substrates, seagrass meadows promote sediment accretion. Other authors have studied sediment resuspension in laboratory experiments (Ros et al., 2014; Zhang et al., 2018; Zhang and Nepf, 2019). Ros et al. (2014), for example, found that the presence of vegetation produced a decrease in resuspension and an increase in sediment deposition compared to bare seabeds. Sediment resuspension is reduced in dense model canopies because of the attenuation of the turbulent kinetic energy (*TKE*) (Gacia et al., 1999; Ros et al., 2014; Zhang et al., 2018; Bos et al., 2007). However, none of these studies quantifies the amount of sediment particles captured by plant leaves or how particles settling onto the seabed is enhanced by the presence of vegetation.

Hendricks et al. (Hendriks et al., 2008) did, however, find that there was a reduction in resuspended sediments within a seagrass canopy compared to bare or eroded grasslands, not only because of reduced hydrodynamic energy, but also because of reduced particle transport due to the energy loss caused by collisions with seagrass leaves. Different rates of reduction in the suspended sediment were also found for different types of *Caulerpa* sp. And seagrass canopies (Hendriks et al., 2010), indicating the role the distinct architectures found within the canopy has in the behaviour of suspended particles. Furthermore, the particle retention by a single cylindrical collector was also quantified and found to increase as the diameter of the collector increased (Palmer et al., 2004). Short and Short (Short et al., 1984) also found a smaller overall turbidity in seagrasses with higher leaf surface area, indicating the potential role the leaves have in reducing water turbidity. In their study, however, no quantification of the sediment deposited on the leaves was carried out. Terrados and Duarte (2000) conducted experiments with leaf detritus samples situated within a seagrass bed and on an unvegetated bed and demonstrated that seagrasses reduce particle resuspension compared to bare sandy beds. Lovelock et al. (2014) found that, because of a higher sediment input in saltmarshes compared to areas of mangroves, a greater accumulation of carbon occurred in the saltmarshes. Howe et al. (2009) also found a higher carbon sequestration in undisturbed saltmarshes compared to disturbed saltmarshes, with the increase in the carbon sequestration in undisturbed saltmarshes being driven by greater rates of vertical accretion. Finally, Agawin and Duarte (2002) studied the capture of particles by seagrass leaves in the field and observed that some of the suspended particles were phagocyted by the seagrass epiphytes found on the leaves of the plants (Agawin and Duarte, 2002). However, in their study they did not explore the role hydrodynamics play in capturing particles.

Despite the availability of all these studies concerning particle dynamics within a seagrass meadow, there are still no studies that address and quantify the effect of the canopy density and the trapping (capturing) of particles by seagrass leaves from allochthonous sources under different hydrodynamic conditions. Therefore, and considering that the fate of allochthonous particle sedimentation in seagrass canopies is not yet fully understood, or that most current findings have been obtained from field observations, the aim of this study was to identify and quantify the role seagrasses have in capturing sediments. To understand the ecological implications, laboratory experiments were carried out to: i) study how sediment particles of different sizes are trapped by plant leaves under different hydrodynamic conditions, ii) examine the suspended sediment concentration within and above the canopy and iii) determine the sedimentation on the seabed of different sized particles. Special attention was paid to the behaviour of the particle sizes for both particle trapping by plant blades, and sedimentation onto the seabed.

2. Methodology

2.1. The flume

The study was carried out in a methacrylate flume (600 × 50 × 50 cm; Fig. 1) with a mean water depth of $h = 30$ cm (Table 1). A vertical flap-type wavemaker was driven by a variable-speed motor at two frequencies (0.7, 1.2 Hz) and four strokes (12, 14, 16, and 18 cm). The wave lengths (λ) were calculated using the dispersion equation by Lowe et al. (Le Méhauté, 1976), as $\lambda = 2.43$ m for $f = 0.7$ Hz and $\lambda = 1.03$ m for $f = 1.2$ Hz. These wave conditions, $\lambda/20 < h < \lambda/2$, corresponded to transitional water waves like those typically found in coastal regions (Serra et al., 2018) with the presence of seagrasses. The waves produced had amplitudes in the range A = 2–4 cm. Therefore, $2A/\lambda = 0.08$, which is below the threshold of 0.14 and corresponds to breaking waves. However, while these waves fell far from the linear Stokes waves, they did correspond to third order Stokes waves, i.e., closer to the breaking limit than linear waves (Le Méhauté, 1976). Third order Stokes waves have been found to produce instabilities at the water surface (in the form of spilling) for $2A/\lambda = 0.10$, thus producing turbulence that is transported downwards in the water column (Iafrati, 2011). The waves used here had $2A/\lambda = 0.08$; close to the threshold found by Iafrati (2011). Therefore, although spilling was not observed through visual inspection, some *TKE* production at the surface could hold. The presence of seagrasses has been found from 1 m to nearly 18 m depths depending on the light attenuation (Duarte, 1991). From these above-mentioned considerations, the scaling of the vegetation in the flume could represent the behaviour of seagrasses in coastal areas. The combination of frequencies and strokes yielded eight wave amplitudes (A = 1.5, 2.0, 2.2, 3.0, 5.0, 5.6 cm). A plywood beach with a slope of 1:3 and covered with a 7 cm thick layer of foam rubber was positioned at the end of the flume to eliminate wave reflection (Pujol et al., 2013b; Pujol and Nepf, 2012). The wavemaker was situated at x = 0 cm in the longitudinal direction, the centre of the tank at y = 0 cm in the lateral direction, and the flume bed at z = 0 cm in the vertical direction.

To mimic the injection of sediment particles from an allochthonous source, a methacrylate pipe (*Internal diameter, ID* = 3 cm, length = 300 cm) with 43 evenly distributed injectors (*ID* = 0.5 cm, length = 8.6 cm, 7 cm apart) was used to inject sediment-laden water (see Section 2.3) into the flume. The end of each injector was covered with a 1 mm mesh to slow down injection rates. The injection pipe was situated outside the water column so that the injectors protruded 5 cm into the water surface as the injection was carried out.

Throughout this study, an allochthonous sediment source is considered as the sediment input from outside the meadow. In the discussion, the results obtained will be compared to other studies carried out on the resuspension of sediment already deposited on the seabed, i.e., not coming from outside the meadow and therefore considered as autochthonous sediment.

2.2. The canopy

Each plant in the canopy was made up of eight 0.075 mm-thick polyethylene canopy leaf blades attached to PVC dowels that had been randomly inserted into a perforated baseboard ($L = 250$ cm (Pujol et al., 2013a),). The rigid dowel extended 1 cm above the bed (Zhang et al., 2018) and the canopy leaf blades were geometrically and dynamically

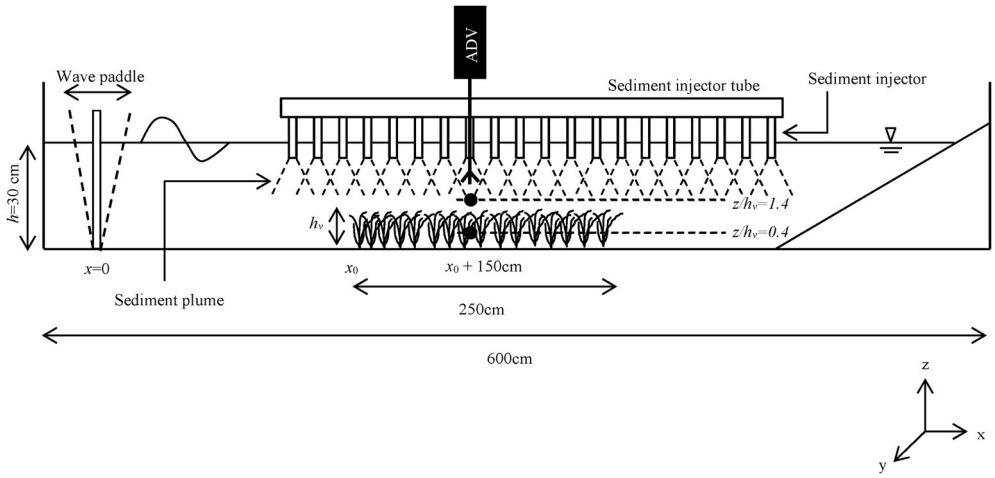

Fig. 1. A lateral view of the experimental setup. Experiments were conducted in a 600 × 50 × 50 cm long flume, with a mean water depth of 30 cm. The model canopy was 250 cm long and canopy height was $h_v = 14$ cm. Filled circles show where both hydrodynamics and sediment measurements were taken. The triangle at the water-air interface represents the water level in the flume.

Table 1
Nomenclature table.

Variable	Units	Definition	Variable	Units	Definition
A	cm	wave amplitude	SPF	%	solid plant fraction
a	cm^2	frontal area	SW	μL	suspended sediment within the canopy ($z/h_v = 1.4$)
ad	non-dimensional	fractional volume occupied by plants	t	min	time
A_{inj}	m^2	injection area	TKE	$cm^2 \cdot s^{-2}$	turbulent kinetic energy
A_w	cm	wave excursion length	T_s	min	time of the steady state
A_w/S_b	non-dimensional	ratio of wave excursion to plant-to-plant distance between blades	u	$cm \cdot s^{-1}$	Eulerian velocity in the x direction
B_o	$m^2 \cdot s^{-3}$	buoyancy flux	u'	$cm \cdot s^{-1}$	turbulent velocity
c	%	particle concentration	U_c	$cm \cdot s^{-1}$	steady velocity associated with the current
c_0	$\mu L \cdot L^{-1}$	initial sediment concentration	U_i	$cm \cdot s^{-1}$	instantaneous velocity
c_p	$\mu L \cdot L^{-1}$	concentration of sediment attached to blades	$U_i(\phi)$	$cm \cdot s^{-1}$	instantaneous velocity according to the phase
c_s	$\mu L \cdot L^{-1}$	suspended sediment concentration at steady state	U_w	$cm \cdot s^{-1}$	wave velocity
c_t	$\mu L \cdot L^{-1}$	suspended sediment concentration with time	U_w^{rms}	$cm \cdot s^{-1}$	orbital velocity
d	cm	blade diameter	v	$cm \cdot s^{-1}$	Eulerian velocity in the y direction
D	m	Injector ID	V_{IN}	%	total volume of particles injected into the flume
$D50$	μm	representative particle diameter	V_{SB}	%	volume of sediment settled to the bed
d_p	μm	particle diameter	V_{SC}	%	volume of suspended sediment inside the canopy ($z/h_v = 0.4$)
f	Hz	wave frequency	Vs_P	%	volume of sediment captured by the plants
g	$m \cdot s^{-2}$	gravitational acceleration	V_{SW}	%	volume of suspended sediment above the canopy ($z/h_v = 1.4$)
h	cm	water height	w	$cm \cdot s^{-1}$	Eulerian velocity in the z direction
h_v	cm	canopy height	w_o	cm·s	injection velocity
ID	cm	inner diameter	x	cm	longitudinal direction
L	cm	canopy length	$x=0$	cm	position of the wave paddle
L_M	cm	length scale	x_0	cm	initial position of the canopy
M_o	$m^4 \cdot s^{-2}$	volume flux	y	cm	lateral direction
n	$stems \cdot m^{-2}$	canopy density	z	cm	vertical direction
n_b	blades	number of blades	z/h_v	non-dimensional	measurement position
n_{inj}	injectors	number of injectors	α_w	non-dimensional	ratio of U_w
P_C	%	partition coefficient of V_{SP} and V_{SC}	β_w	non-dimensional	ratio of TKE
Q	$m^3 \cdot s^{-1}$	injection flow	Δb_o	$m \cdot s^{-2}$	buoyancy of the resting plume fluid
Q_o	$m^4 \cdot s^{-3}$	momentum flux	λ	m	wave length
S_b	cm	blade-to-blade distance	ρ_s	$kg \cdot m^{-3}$	water density
SB	μL	sediment settled to the bed	ρ_w	$kg \cdot m^{-3}$	sediment density
SC	μL	suspended sediment within the canopy ($z/h_v = 0.4$)	ϕ	radians	wave phase
SP	μL	sediment attached to plants	ω	$radians \cdot s^{-1}$	angular frequency
			k	$radians \cdot cm^{-1}$	spatial frequency

similar to those of *Posidonia oceanica* (Pujol et al., 2013a; Ghisalberti and Nepf, 2002; Folkard, 2005). The canopy height was $h_v = 14$ cm, however, the effective height when the leaf blades were bent by the waves was $h_v = 13 \pm 1$ cm. The initial position of the vegetation (x_0) was situated 100 cm from the wavemaker (Fig. 1). The canopy density was quantified using the solid plant fraction (SPF) defined as:

$$SPF\ (\%) = 100n\pi\left(\frac{d}{2}\right)^2 \quad (1)$$

where n is the number of stems per unit area and d is the stem diameter (1 cm). Five *SPF*s were used (0%, 1%, 2.5%, 5% and 7.5%), which corresponded to canopy densities n = 0, 127, 318, 637 and 955 stems·m^{-2} (Fig. 2) which fall within the range 78–1000 stems·m^{-2} found in the field (Hendriks et al., 2008; Ghisalberti and Nepf, 2002; Folkard, 2005; Zhang and Nepf, 2008; Goring and Nikora, 2002). *SPF* = 0% corresponded to unvegetated beds. Two frequencies and eight wave amplitudes varied across the five *SPF*s resulted in a total of 40 experiments (Table 2), each 90 min in duration.

The fractional volume occupied by the plants (ad) for each canopy density was calculated as the frontal area of the plant per unit volume, a, multiplied by the stem diameter, d (Zhang and Nepf, 2008). Greyscale photographs taken from the top of the canopy were analysed to calculate canopy cover in the absence of wave motion (Serra et al., 2018). The five canopy densities corresponded to a canopy cover of 0, 37.4, 52.1, 70.6 and 80.9% (Fig. 2) and the photographs determining the cover were taken in the absence of wave motion. Canopy cover followed a non-linear trend with the fractional volume (Fig. 2e) cover = 207*$ad^{0.4}$, indicating that full cover (100%) occurred at ad = 0.16, corresponding to an *SPF* of 12.5% and a canopy density of 1592 stems·m^{-2}.

2.3. Measuring velocities

The Eulerian velocity field was defined as (u, v, w) in the (x, y, z) directions, respectively. The three components of velocity were recorded (at a frequency of 50 Hz over 10 min) with a downwards-looking Acoustic Doppler Velocimeter (16-MHz MicroADV, Sontek). The ADV measures at a distance of 5 cm from the probe tip, and with a sampling volume of 0.09 cm^3. Beam correlations less than 80% were discarded and spikes were removed (Pujol et al., 2013a; Goring and Nikora, 2002). The number of spikes increased slightly with the presence of the plants and the canopy density compared with the unvegetated case. The percentage of spikes was from 0.33% for the unvegetated case to 0.77% for the most densely vegetated case.

To eliminate the lower order spatially periodic variation in wave and velocity amplitude associated with wave reflection (Pujol et al., 2013a; Luhar et al., 2010), the longitudinal velocity was measured at an antinode. The model canopy was then shifted longitudinally along the flume to ensure measurements were taken 150 cm from the canopy edge. For the densest canopy experiments, some plants were removed and re-inserted into nearby holes to avoid blocking the ADV beams (Zhang et al., 2018; Zhang and Nepf, 2019; Pujol et al., 2010, 2013b; Colomer et al., 2017).

2.4. Velocity and turbulent kinetic energy analysis

For oscillatory flows, the instantaneous velocity, $U_i(t)$, can be decomposed as:

$$U_i(t) = U_c + U_w + u'. \quad (2)$$

where U_c is the steady velocity associated with the current, U_w is the unsteady wave motion which represents spatial variations in the phase-averaged velocity field, and u' is the turbulent velocity, that is, the instantaneous velocity fluctuation in the x-direction. U_c is the phase-averaged velocity:

$$U_c = \frac{1}{2\pi}\int_0^{2\pi} U_i(\phi)\partial\phi \quad (3)$$

where $U_i(\phi)$ is the instantaneous velocity according to the phase (Luhar et al., 2010; Lowe et al., 2005). Wave velocity, U_w, was obtained by using a phase averaging technique. The Hilbert transform was used to average oscillatory flow velocities with a common phase (Ros et al., 2014; Pujol et al., 2013b). The root mean square (rms) of $U_i(\phi)$ was considered as the characteristic value of the orbital velocity U_w^{rms} (U_w hereafter) at each depth, and was calculated according to:

$$U_w^{rms} = \sqrt{\frac{1}{2\pi}\int_0^{2\pi}(U_i(\phi) - U_c)^2\partial\phi} \quad (4)$$

For cases WP5 and SFV37, vertical profiles of the velocity were taken from which the wave velocity and turbulent kinetic energy profiles were calculated (Fig. 3). The wave velocity decreased from the layer above the canopy to the bed. From the vertical profile of the wave velocity, two vertical regions were differentiated: the above-canopy layer and the within-canopy layer (Fig. 3a). In the above-canopy layer, the wave velocity was the highest with similar results compared to the without-

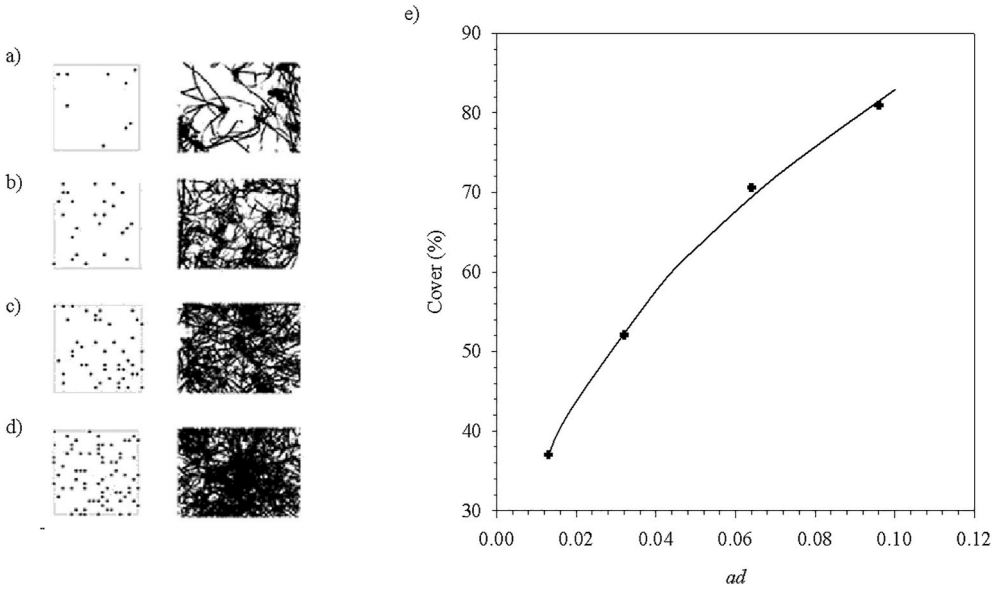

Fig. 2. Plant distribution for the different *SPF*s a) 1%, b) 2.5%, c) 5%, and d) 7.5% on the PVC bases (left panels) and black and white digitized photography (right panels). e) is the relationship between the canopy cover (%) and the volume plant fraction (ad).

Table 2
Summary of the wave and vegetation parameters for each experiment.

Run	Canopy model	*SPF* (%)	*n* (stems·m^{-2})	Coverage (%)	*ad*	S_b (cm)	*F* (Hz)	λ (m)	*A* (cm)	A_w (cm)
WP1	Without vegetation	0	0	0	0		0.7	2.43	2.0	0.91
WP2									2.2	1.43
WP3									2.0	2.02
WP4									1.5	2.16
WP5							1.2	1.03	3.0	1.82
WP6									3.2	1.63
WP7									5.0	1.96
WP8									5.6	2.55
SFV9	Submerged flexible vegetation model	1	127	37	0.013	3.14	0.7	2.43	2.0	0.98
SFV10									2.2	0.65
SFV11									2.0	2.70
SFV12									1.5	2.18
SFV13							1.2	1.03	3.0	2.70
SFV14									3.2	1.24
SFV15									5.0	1.21
SFV16									5.6	1.11
SFV17		2.5	318	52	0.032	1.98	0.7	2.43	2.0	1.43
SFV18									2.2	0.80
SFV19									2.0	2.82
SFV20									1.5	2.83
SFV21							1.2	1.03	3.0	1.52
SFV22									3.2	1.39
SFV23									5.0	1.66
SFV24									5.6	1.77
SFV25		5	637	71	0.064	1.40	0.7	2.43	2.0	0.45
SFV26									2.2	1.18
SFV27									2.0	1.54
SFV28									1.5	1.51
SFV29							1.2	1.03	3.0	1.39
SFV30									3.2	1.61
SFV31									5.0	1.55
SFV32									5.6	1.96
SFV33		7.5	955	81	0.096	1.14	0.7	2.43	2.0	1.09
SFV34									2.2	0.61
SFV35									2.0	0.75
SFV36									1.5	1.56
SFV37							1.2	1.03	3.0	1.67
SFV38									3.2	1.82
SFV39									5.0	1.69
SFV40									5.6	1.72

plants case. In the within-canopy layer, the velocity decreased gradually with depth until $z = 5$ cm ($z/h_v = 0.4$) where the wave velocity remained nearly constant down to the bottom. In this layer, the velocity in the presence of plants was lower than that in the without-plants case.

The turbulent velocity was obtained by:

$$u' = U_i - U_c - U_w \tag{6}$$

where U_c and U_w were calculated by Eqs. (3) and (4). The same methodology was used to calculate the other two turbulent velocity components (v' and w').

The turbulent kinetic energy (*TKE*) was calculated following Ros et al. (2014) as:

$$TKE = \frac{1}{2}\left(u'^2 + v'^2 + w'^2\right) \tag{7}$$

where $< >$ denotes the time average.

Like U_w, the *TKE* decreased with depth (Fig. 3b) and the same two vertical layers (above-canopy and within-canopy) can be distinguished. The above-canopy layer presented similar *TKE* for both the with and without-plants experiments. Within the canopy, the *TKE* decreased compared to the without-plants experiments. From the results of the vertical profiles of both U_w and *TKE*, the depth of $z = 5$ cm was considered representative of the hydrodynamics of the within-canopy layer, and the depth of $z = 20$ cm representative of the hydrodynamics of the above-canopy layer. Therefore, for the rest of the experiments carried out, the current velocity was measured at these two vertical positions: $z = 20$ cm ($z/h_v = 1.4$, above the canopy) and $z = 5$ cm ($z/h_v = 0.4$, within the canopy). Within the canopy layer (at $z/h_v = 0.4$), the mean flow velocity was $U_c = -0.04$ cm s^{-1} and -0.10 cm s^{-1} for non-vegetated experiments and for the wave frequencies of $f = 0.7$ Hz and $f = 1.2$ Hz, respectively. For experiments with vegetation, and at the same depth, the mean flow velocity among all the experiments as $U_c = -0.22$ cm s^{-1} for $f = 0.7$ Hz and -0.25 cm s^{-1} for wave frequencies $f = 1.2$ Hz. These flow velocities were negative in all the cases, indicating that they were directed towards the wave maker. They have lower values than those found in the experiments of (Luhar et al., 2010), where they used a paddle type wave maker with frequencies of 0.5 Hz and U_c at this depth was directed towards the beach. In this present study, a flap-type wave maker was used, and higher wave frequencies were considered. This study gives similar results and directions for U_c as those found by (Pujol et al., 2013b) for the same type of wave maker and frequencies of 1 Hz and 1.4 Hz.

2.5. Sediment-laden injection

A synthetic dust powder (ISO 12103–1. A4 Coarse, Powder Technology Inc. Burnsville) was used as the sediment in the experiments. The volumetric concentrations of suspended sediment (in μL·L^{-1}) were analysed using the LISST-100X (Laser In-Situ Scattering and Transmissometry, Sequoia Scientific, Inc, Bellevue, WA) particle size analyser. The LISST-100X consists of a laser beam and an array of detector rings of progressive diameters which allow the light received at the scattering angles of the beam to be analysed. The device measures particle volume concentrations for 32 size-classes, (logarithmically distributed in the size range of 2.5–500.0 μm), using a procedure based on the diffraction

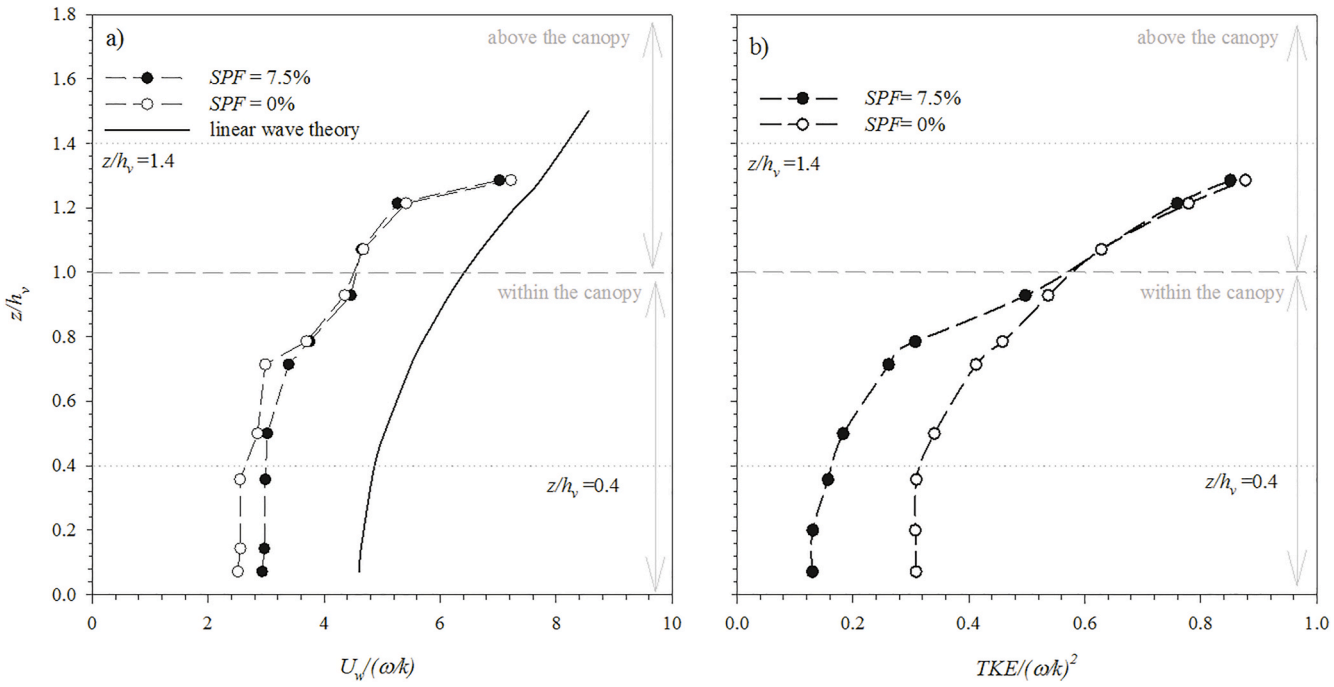

Fig. 3. Vertical profiles of both the wave velocity $U_w/(\omega/k)$, where $\omega = 2\pi f$ and $k = 2\pi/\lambda$(a) and the turbulent kinetic energy $TKE/(\omega/k)^2$ (b) for $SPF = 0\%$ (unfilled circles), $SPF = 7.5\%$ (filled circles) and the linear wave theory (solid line). The dashed line shows the top of the plant blades and the dotted lines show the level where the measurements were taken. The vertical axis represents the non-dimensional depth z/h_v.

theory of light. The LISST-100X has been found to perform well when determining particle size distribution and concentration for both organic (Serra et al., 2001) and inorganic particles (Serra et al., 2002a, 2002b) suspended in water. This instrument can be used *in situ* in the field, where it can be submerged in the water, or it can be employed in the laboratory to measure small samples by using a measuring chamber. For laboratory use, the water sample has to have a volume between a minimum of 80 ml (to ensure the detector is completely covered) and a maximum of 100 ml (the maximum volume of the measuring chamber). The particle size distribution of the sediment used was bimodal, with fine particles, 2.5–6.0 μm in diameter, corresponding to strongly cohesive clay and very fine silts with a median $D50 = 3.78$ μm and making up 30% of the sediment, and coarse particles, 6.0–122 μm in diameter, corresponding to weakly cohesive fine to coarse silts and small sand

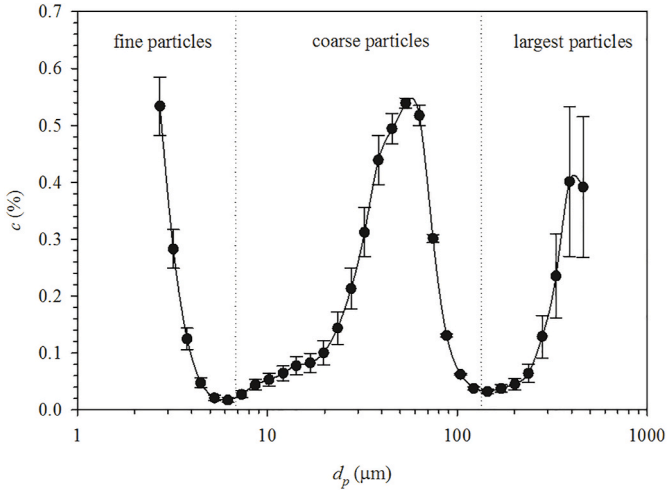

Fig. 4. Sediment particle distribution in %. Three different particle sizes are shown: fine particles below 6 μm, coarse particles between 6 and 122 μm, and the largest size particles over 122.0 μm.

particles with a median of $D50 = 27.6$ μm making up 70% of the sediment (Fig. 4). The concentration of the particles in each size-class was calculated by the sum of the volume concentrations of the particles ranging between 2.5 and 6.0 μm for the fine particles and between 6.0 and 122.0 μm for coarse particles (Fig. 4). The particle concentration will be expressed in volume concentrations in the whole manuscript to mitigate for the quantity of fine particles in every sediment mixture being higher than the coarse particles.

Before the injection, the wavemaker was started and left to run for 60 min to allow the system to reach equilibrium. After this time had elapsed, the particle-laden flow to be used in the injection was prepared with an initial volume (2 L) of sediment suspension (with a concentration of 40 g L^{-1}) introduced into one end of the sediment-injection pipe. The injection pipe was situated at $y = 0$ along the axis of the flume (Fig. 1). While introducing the sediment into the pipe, the injectors faced upwards to avoid any uncontrolled spillage. Once the pipes had been filled with the sediment suspension, they were closed and then turned to face downwards with their ends protruding 5 cm below the water surface, thus producing an even release of suspended sediment along the flume. After 18 s, individual injector plumes started to merge. The injection of sediment lasted less than 1.5 min. The sediment mass from the injection produced a total suspended sediment concentration (c_s) in the flume within the range 5–14 μL L^{-1}, which coincides with the typical sediment concentration discharges, 4–400 μL L^{-1}, of river plumes in coastal waters (Mulder and Syvitski, 1995). A river plume in the Bay of Bengal was found to discharge concentrations in the range of 0.4 μL L^{-1} to 20.7 μL L^{-1} (Sridhar et al., 2014), also in a range similar to that in the present study.

The length scale, L_M (Colomer et al., 1999), was used to calculate the 'plume' or 'jet' nature of the injection. L_M indicates the distance up to where the injected fluid behaves as a jet and was calculated as:

$$L_M = \frac{M_O^{3/4}}{Q_O^{1/2}} \tag{9}$$

where M_o was the volume flux and Q_o was the momentum flux. *Mo* was calculated as:

$$M_O = \frac{\pi D^2 w_o^2}{4}. \quad (10)$$

where D is the inner diameter of the injectors and w_o is the injection velocity, calculated as:

$$w_o = \frac{Q}{n_{inj}\, A_{inj}}. \quad (11)$$

where Q is the injection flow, n_{inj} is the number of injectors and A_{inj} is the injector area.

Q_o was calculated as:

$$Q_o = \frac{\pi D^2 B_o}{4} \quad (12)$$

where Bo is the buoyancy flux per unit area, calculated as:

$$B_o = \Delta b_o w_o \quad (13)$$

where Δb_o is the buoyancy of the resulting plume fluid, calculated as:

$$\Delta b_o = \frac{(\rho_s - \rho_w) g}{\rho_w} \quad (14)$$

where $\rho_s = 2500$ kg m^{-3} is the sediment density, $\rho_w = 1000$ kg m^{-3} is the water density and $g = 9.8$ m s^{-2} is the gravitational acceleration.

Merging equations (9)–(14) resulted in $L_M = 0.025$ cm. Therefore, the injection behaved like a jet for distances up to 0.025 cm from the injector and then plume-like once it got further away than that. As the water depth was 30 cm and the plants extended up 14 cm, the possibility the injectors being a source of turbulence within the canopy was discarded and the plume character of the injector was demonstrated. In addition, a test for the effect the injection has on the *TKE* measurements was carried out. That is, the *TKE* was measured with and without the injection. The *TKE* with the injection increased by 5.5%, which is within the standard deviation measured for the *TKE*. In addition, the injection time was less than 1.5 min, representing 1.2% of the total running period of the sediment study. Therefore, any effect the injection might have had on the measuring point was disregarded.

2.6. Sediment measurements

In the first test, two transversal points (situated 25 cm apart) and two longitudinal (1 m apart) were considered for the particle concentration measurements and confirmed that, after 1.5 min of injection, the suspended sediment was not only homogeneously mixed in both the longitudinal and transversal directions of the flume with maximum differences of 0.06 μL L^{-1} but was also below the standard deviation obtained for the measurements of the concentration at one single point (of 0.20 μL L^{-1}). Therefore, the samples of sediment were taken at $y = 0$ and at the same x-position where the hydrodynamics were measured (x = 150 cm from the edge of the canopy). The concentration of suspended sediment c_t (μL·L^{-1}), was measured at the same water depths ($z/h_v = 0.4$ and at $z/h_v = 1.4$) considered representative for the hydrodynamics in both the above-canopy and the within-canopy layers (Fig. 3a and b). Water samples, 20 mL in volume, were collected with a pipette from these two depths at different time steps $t = 1$, 5, 15, 30, 45, 60 and 90 min, and analysed for suspended sediment concentration. As the samples were not returned to the flume, this represented a total volume decrease of 280 mL (a 0.03% decrease in the total volume of the water volume) during the running time of the experiment. This change in the water volume produced a negligible change in the water height (<0.05 cm). The time evolution for the sediment concentration, c_t, decreased and reached the steady state (c_s) at $t = 60$ min (T_s, Fig. 5). At the end of the experiment ($t = 90$ min), ten model plants were gently removed from different evenly separated positions within the meadow and introduced into a beaker with a volume of 80 mL of water. The plants were then stirred in the fluid to remove the sediment trapped by the surface of the blades, after which particle concentration (c_p) was analysed with the particle size analyser (LISST-100X).

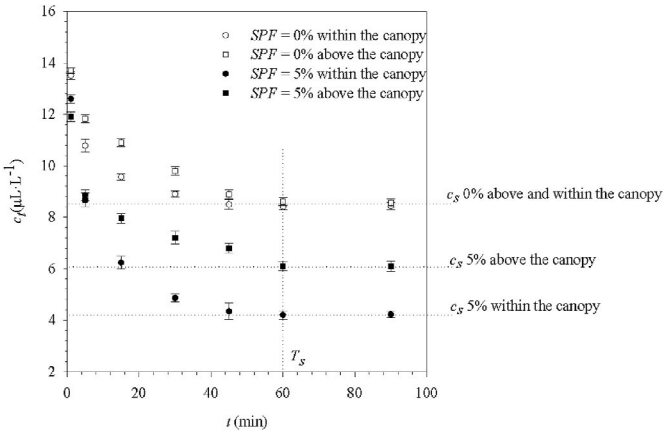

Fig. 5. Decline in suspended sediment concentration, c_t, with time, comparing experiments with canopy (*SPF* 5%) and at the equivalent heights in experiments without canopy (*SPF* 0%). Sediment concentrations were measured above the canopy ($z/h_v = 1.4$) and inside the canopy ($z/h_v = 0.4$). The vertical dashed line indicates the time (T_S) to reach steady state conditions, while the horizontal dashed lines indicate steady state sediment concentrations (c_s).

2.7. Sediment mass balance

A conceptual model was developed for the canopy system with four sediment compartments based on the hydrodynamics (Fig. 3): sediment suspended within the canopy (*SC*), sediment suspended in the water above the canopy (*SW*), sediment attached to the leaf blades (*SP*), and sediment settled at the bottom of the tank (*SB*). For suspended sediments, the concentrations measured within each compartment were mutiplied by the volume of the compartment to estimate the volume (in μL) of the suspended sediments in that compartment. To determine the total volume of sediment attached to the plant blades (μL), measured particle concentrations were normalised per plant and then multiplied by the total number of plants in the canopy (which varied with *SPF*). The volume of particles settled to the bottom was not directly measured, instead it was calculated as the difference between the total volume injected and the sum of the suspended particle volume and the volume attached to plants.

V_{IN} is the total volume injected, distributed in the region occupied by the canopy, calculated by multiplying the injected sediment mass by the volume of the canopy and divided by the total volume of the flume. Finally, the injected mass was converted to volume units using the sediment density (2500 kg m^{-3}). The injected volume was fractionated into fine and coarse particles using the previously-determined particle size distribution.

A volume balance was then determined as:

$$V_{IN}^F = V_{SC}^F + V_{SW}^F + V_{SP}^F + V_{SB}^F \quad (15)$$

where V_{IN}^F is the volume of fine particles injected above the canopy, V_{SC}^F is the volume of suspended fine sediment inside the canopy, determined at $z/h_v = 0.4$, the volume inside the canopy corresponded to the water volume, which is inside the area and height of the vegetation, V_{SW}^F is the volume of suspended fine sediment in the water above the canopy, determined at $z/h_v = 1.4$, V_{SP}^F is the volume of sediment captured by the plants, and V_{SB}^F is the volume of fine sediment settled to the bottom. An equivalent volume balance was made for coarse sediments:

$$V_{IN}^C = V_{SC}^C + V_{SW}^C + V_{SP}^C + V_{SB}^C \quad (16)$$

3. Results

Differences in the turbulent kinetic energies were found between the bare substrate and sparse and dense canopies. The results of the turbulent kinetic energy averaged over all the experiments carried out with different wave amplitudes and the same frequency and *SPF* are referred to as the mean turbulent kinetic energy (*<TKE>*). The *<TKE>* decreased gradually with the canopy cover for both wave frequencies. Considering the error margin, no differences in the *TKE* were obtained between the two frequencies studied (0.7 and 1.2 Hz) (Fig. 6). The reduction in the *<TKE>* for sparse canopies and dense canopies ranged from 14% to 35% to that of the *<TKE>* of the bare substrate.

The suspended sediment concentrations at steady state, c_s, for both fine and coarse particles, were linearly dependent on *TKE* (Fig. 7a). Since the *TKE* depended on the cover, the average of the steady state concentrations ($<c_s>$) over the same cover experiments for both fine and coarse particles decreased as canopy cover increased (Fig. 7b). The sediment trapped by the surface of the blades of each plant, c_p, was also analysed, (as described in Methods), and quantified as the concentration of sediment in the wash-off liquid. The coarse particles captured by each plant showed similar linear relationships with *TKE* as those observed for the steady state suspended sediment concentrations (Fig. 7c) In contrast, the concentration of fine particles trapped by the blades of the plants was independent of the *TKE* (Fig. 7c). The average of the particle concentration trapped by the plants in the whole canopy ($<c_p>$) was calculated for each canopy cover and increased as the canopy cover increased (Fig. 7d).

For all the experiments, the volume of fine and coarse sediment particles was calculated as outlined in the methodology. For example, the volume of particles suspended within the canopy was calculated by multiplying the concentration of suspended particles at $z = 0.4\ h_v$ by the volume of the region occupied by the canopy. For the non-vegetated case, the volumes of the fine V_{SC}^F(Fig. 8a), and coarse, V_{SC}^C (Fig. 8b) particles that remained in suspension in the bottom portion of the water where the canopy was present for the vegetated cases, were greater than those of the vegetated cases. Also, in both cases the volumes of the fine V_{SP}^F (Fig. 8a) and coarse V_{SP}^C (Fig. 8b) particles trapped by plant blades increased as the cover increased. The increase in the particles trapped by plant blades in the whole canopy, V_{SP}, coincided with a decrease in V_{SC}. The volume of suspended sediment above the canopy for both the fine and coarse particles (V_{SW}^F and V_{SW}^C) decreased with the increase in canopy cover. Finally, the sedimentation (V_{SB}) to the bottom increased as the canopy density increased and ranged from 75% to 80% for fine particles over the total volume of fine particles and from 57% to 60% for coarse particles over the total volume of coarse particles (following equations (15) and (16)). For the non-vegetated cases, the sedimentation to the bottom was lower than that for vegetated cases, around 70% for fine particles and around 46% for coarse particles (Fig. 8a and b). In each case, the percentage is given over the total amount per each particle range.

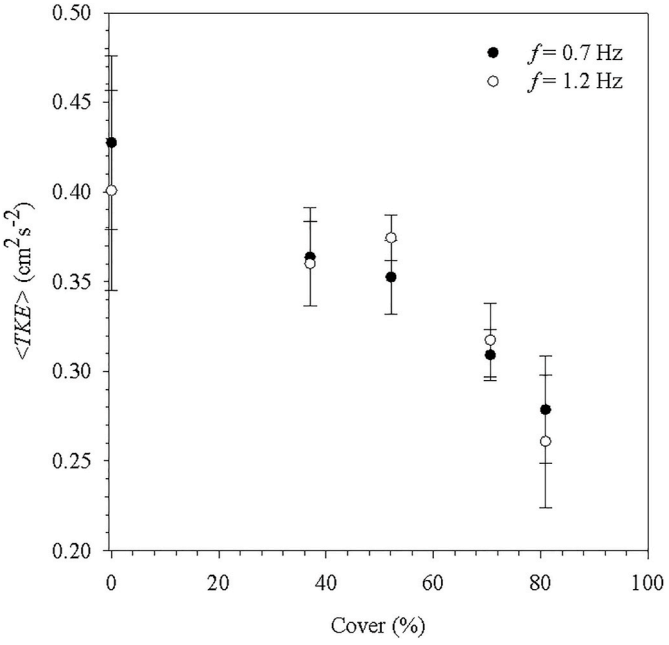

Fig. 6. *TKE* values within the canopy averaged over the experiments, *<TKE>* with the same canopy density (*SPF*) versus the canopy cover for both the high frequency (1.2 Hz, unfilled circles) and the low frequency (0.7 Hz, filled circles) experiments.

The partition coefficient (P_C) between the sediment trapped by the plant blades and the suspended sediment inside the canopy (V_{SC}) was calculated as:

$$P_C = \frac{V_{SP}}{V_{SC}} * 100 \tag{17}$$

P_C decreased linearly with *<TKE>* for both fine and coarse particles (Fig. 9a). For *<TKE>* above 0.36 $cm^2 s^{-2}$, corresponding to cover percentages <52%, the P_C for fine and coarse particles did not present any differences. For high canopy covers, the partition coefficient was greater for fine particles (Fig. 9b) than for coarse particles. For the highest cover, P_C was 50% for fine particles, i.e., $V_{SP}^F = 0.5 V_{SC}^F$, which indicates that the volume of particles captured by the leaf blades is half that remaining in suspension inside the canopy. P_C was 30% for coarse particles, i.e., $V_{SP}^C = 0.3 V_{SC}^C$ (Fig. 9b).

4. Discussion

Experiments performed in the laboratory flume showed that allochthonous sediment encountering seagrass canopies can undergo different fates, namely be: i) maintained in suspension above the canopy, ii) maintained in suspension within the canopy, iii) captured by plant blades or iv) settle to the seabed. However, results show that submerged seagrass canopies under oscillatory conditions affect the hydrodynamics and the distribution and transport of sediments mainly by reducing the wave velocity and the turbulent kinetic energy that depends on both canopy density and wave frequency.

4.1. Submerged model vegetation hydrodynamics by oscillatory flow

Submerged canopies were found to attenuate both wave velocity and *TKE* within the canopy, in agreement with (Pujol et al., 2013b) in their laboratory study and the results observed by Gacia et al. (1999) and by Hendriks et al. (2008) in their field studies. The *TKE* attenuation of between 14 and 35% found in this laboratory study, agrees with the 25% reduction in turbulence between bare substrate and *P. oceanica* bed found by Granata et al. (2001) in their field study. The fact that the *TKE* decreased with the canopy cover indicates that dense canopies shelter the seabed. This reduction in the *TKE* produces different distributions of sediment depending on the density of the cover. The decrease in the *TKE* with depth was also found by Zhang et al. (2018), but in their case, the *TKE* in the upper without-plant water layer was lower than in the present study. In laboratory conditions the plant height was $h_v = 14$ cm, wave amplitudes were A = 1.5 cm and 5.6 cm and the periods were $T =$ 1.43 s and 0.83 s. Considering the flume height $H = 30$ cm and shallow field depth cases with $H = 100$ cm a scale factor of 3.3 would apply by using Froude scaling (Islam et al., 2016). Using the Froude scaling, the laboratory studied conditions would represent field waves with amplitudes of $A = 4.95$ and 18.48 cm and periods of $T = 2.59$ s and 1.51 s. Such field conditions might be found in river or lake environments and closed basin estuaries in marine systems (Pascolo et al., 2019; Smith et al., 2001), where particle laden river plumes may have a significant

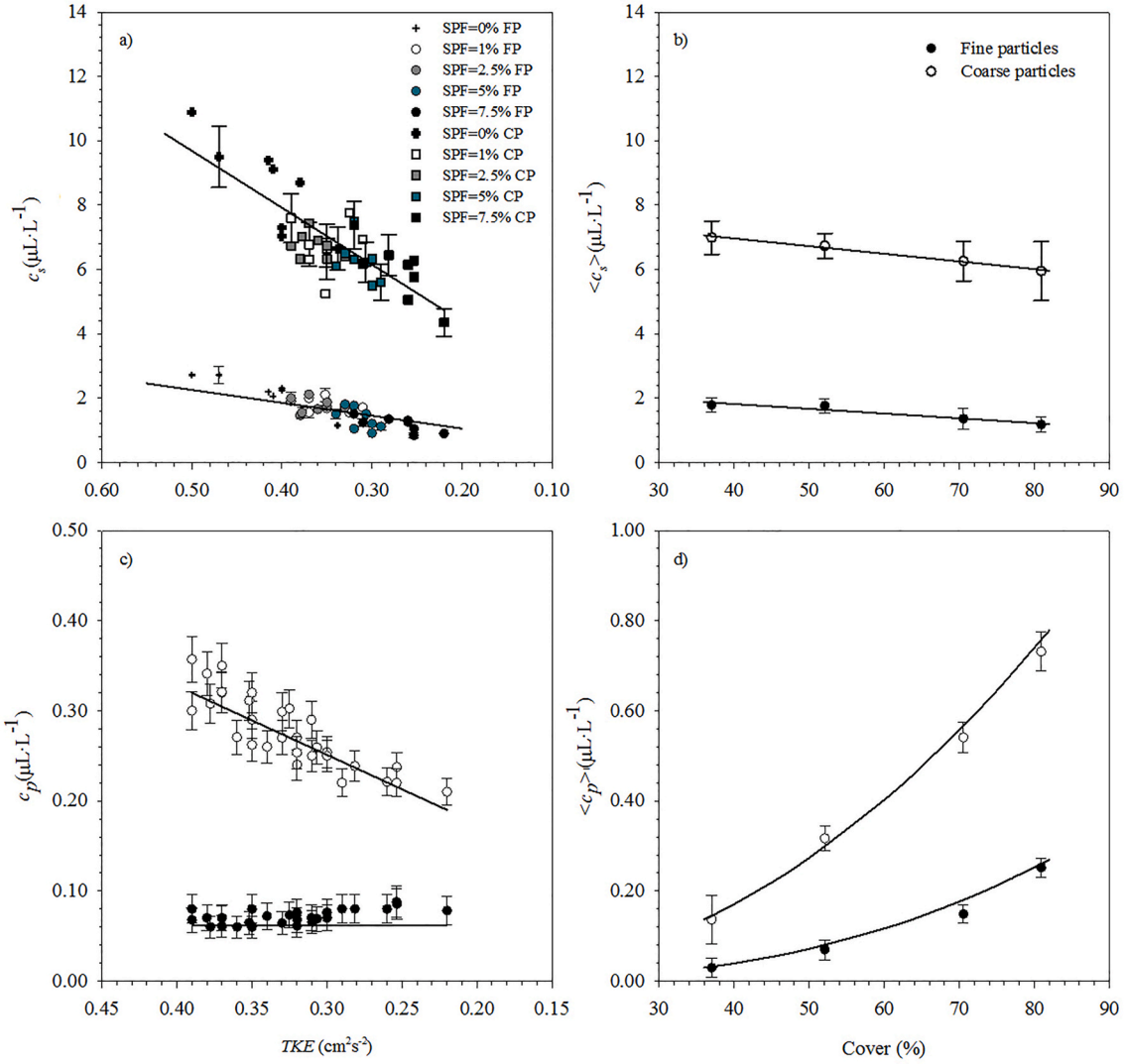

Fig. 7. a) Steady state suspended sediment concentration, c_s, versus *TKE*, with variable *SPF*. Circles correspond to fine particles (FP) and squares to coarse particles (CP). Fine and coarse particles follow a linear trend with the expressions: $c_s = 17.69*TKE+0.84$ (with a $R^2 = 0.681$ and 99% of confidence) and $c_s = 6.69*TKE-0.74$ (with a $R^2 = 0.742$ and 99% of confidence), respectively; b) Steady state suspended sediment concentration averaged over the experiments with the same canopy cover versus canopy cover for fine particles (filled circles) and coarse particles (unfilled circles). The linear trends for fine and coarse particles are: $<c_s> = -0.01*Cover+2.41$ (with a $R^2 = 0.919$ and 95% of confidence) and $<c_s> = -0.02*Cover+7.91$ (with a $R^2 = 0.988$ and 99% of confidence), respectively; c) Sediment captured by each plant c_p, for fine and coarse particles versus *TKE*. Coarse particles follow the linear trend expression: $c_p = 1.23*TKE–0.13$ (with $R^2 = 0.673$ and 99% of confidence); d) Mean sediment concentration captured by all the plants in the canopy averaged over all the experiments with the same canopy cover versus canopy cover for fine and coarse particles. The potential trend expression followed by coarse particles is: $<c_p> = 7*10^{-5}*Cover^{2.11}$ (with $R^2 = 0.994$ and 99% of confidence) and fine particles follow the expression: $<c_p> = 2*10^{-6}*Cover^{2.68}$ (with $R^2 = 0.994$ and 99% of confidence). Vertical error bars represent the standard deviation in the concentration obtained by different measurements of the concentration for the same experiments. In Fig. 7a, only some error bars have been shown to provide a clear plot of the data.

impact (Oey and L Mellor, 1993; Howley et al., 2018).

4.2. Effect of the canopy on the suspended sediment from the allochthonous plume

The concentration of suspended sediment in the water column follows a linear relationship with the *TKE*. High *TKE* corresponds to the sparsest canopies, whereas low *TKE* corresponds to the densest. Therefore, the decrease in the suspended sediment concentration corresponded to the densest canopies. This result is in agreement with the reduction of turbidity found by Short and Short (Short et al., 1984) for a vegetated bed. Consequently, the presence of a seagrass canopy protects seagrass meadows in coastal regions by enhancing the sedimentation. This result has been observed in the field, where a greater sediment deposition was found on the seabeds sheltered by *P. oceanica* in the NE Spanish Mediterranean (Grabowski et al., 2011; Gacia et al., 1999).

4.3. Allochthonous sediment trapped by the blades of an individual plant

This study demonstrated that plant blades trap sediment particles. Sediment trapped by blades in sparse canopies was quantified and compared to that in dense canopies. The sediment concentration trapped by the blades of each plant, (c_p), was higher for coarse particles than it was for fine ones. The concentration of fine particles trapped on the leaf blades of each plant remained constant with the *TKE* and with the canopy density, which may be due to the leaves of the plants easily trapping fine particles until the surfaces become saturated. In contrast, the concentration of coarse particles trapped on the leaf blades of each plant increased with the *TKE*, i.e., decreased with cover. Therefore, for coarse particles the greatest concentration of particles trapped by plant

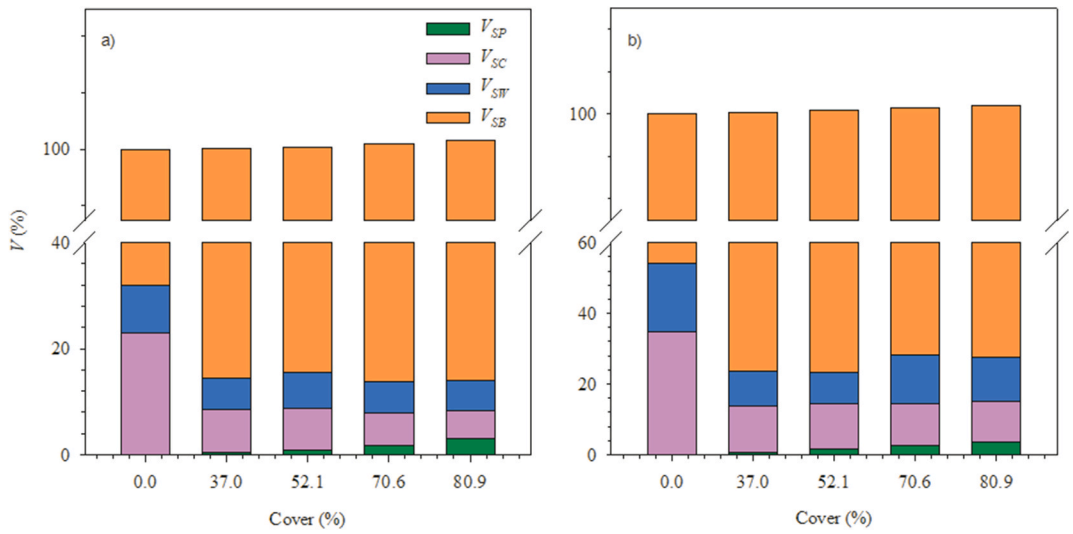

Fig. 8. Sediment volume balance (V) of the volume trapped by the blades (V_{SP}), volume inside the canopy (at $z/h_v = 0.4$) (V_{SC}), volume above the canopy (at $z/h_v = 1.4$) (V_{SW}) for different covers for fine particles (a) and for coarse particles (b), and volume deposited to the bottom (V_{SB}).

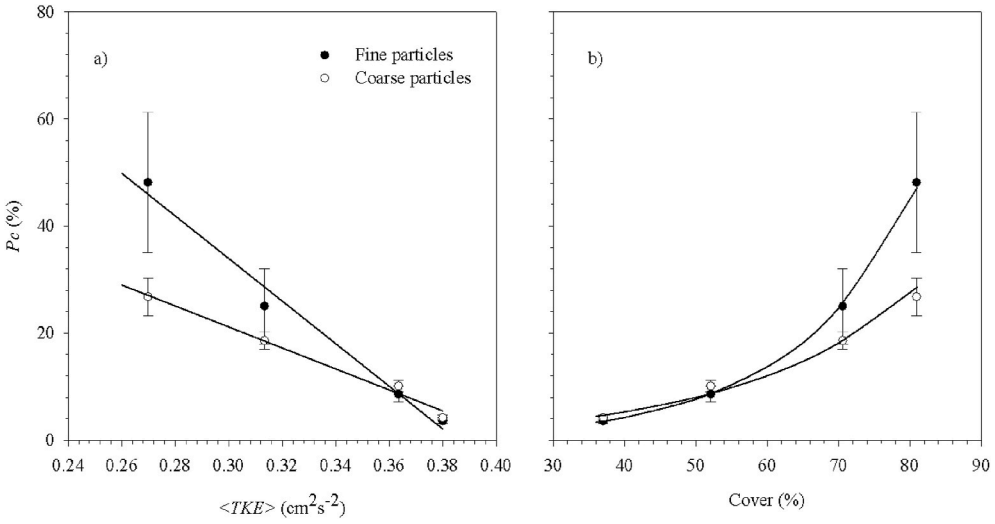

Fig. 9. a) Partition coefficient of the sediment trapped by the blades versus the $<TKE>$ for fine particles (filled circles) and for coarse particles (unfilled circles). $<TKE>$ is the mean value of the *TKE* averaged over the experiments with the same cover. Fine and coarse particles follow a linear trend with the expressions: $Pc = -397.8*<TKE>+153.3$ ($R^2 = 0.981$ and 99% of confidence) and $Pc = -196.2*<TKE>+80.0$ ($R^2 = 0.995$ and 99% of confidence), respectively; b) Partition coefficient for the sediment trapped by blades for the two particle size ranges versus the cover. The relationship between *Pc* and the cover showed an exponential tendency ($Pc = 0.4e^{0.06cover}$, $R^2 = 0.994$ and $Pc = e^{0.04cover}$, $R^2 = 0.987$ for fine and coarse particles, respectively). Error bars represent the standard deviation between the different experiments carried out at the same $<TKE>$ (Fig. 9a) and for the same cover (Fig. 9b).

leaves corresponded to the lowest canopy density. Two possible reasons could explain this result. A first hypothesis is that in sparse canopies there is a reduction in the interaction between leaf blades, whereas in dense canopies the contact between blades can wash off the sediment deposited on the blades of neighbouring plants, thus resulting in cleaner blades. As reported by Gacia et al. (1999) and Hendricks et al. (Hendriks et al., 2008), an increase in the canopy density generates an increase in plant blade friction. The second hypothesis is that sparser canopies have higher *TKE*, thus favouring the contact between particles and blades and resulting in a greater amount of sediment being trapped on the surface of the plant blades. Short and Short (Short et al., 1984) also observed that seabeds covered by plants with blades of leaves with large surface areas produced a greater reduction in the turbidity of the water column compared to seabeds covered by plants with blades that have a small surface area.

4.4. Allochthonous sediment trapped by the overall canopy

Therefore, the decrease in the within-canopy suspended sediment could be attributed to two factors: the capture of suspended particles by plant blades or the particles settling onto the bed. This is consistent with the fact that the presence of plants increases the available surface where particles can settle and so an increase in plant density implies an increase in the available surface.

Agawin and Duarte (2002) observed that particles with diameters around 15 μm were trapped faster by canopy blades than those particles around 1–3 μm. The trapping rates were 0.24 d^{-1} and 0.50 d^{-1} for 15 μm and 3 μm, respectively. At first glance, it would seem that their results do not agree with the results obtained in this study, where a greater sediment volume was found for the coarse particles, however, in converting the volume of particles to the number of particles for a canopy cover of 80.9%, the volume trapped by plants corresponds to a number of particles of 9.44×10^9 and 8.13×10^6 for fine and coarse particles, respectively. Therefore, a larger number of fine particles (as opposed to coarse particles) are trapped by the leaf blades, which is consistent with Agawin and Duarte (2002). This may be caused by the greater cohesiveness of fine particles compared to coarse particles (Grabowski et al., 2011).

In terms of mass balance, the total volume of particles settled to the bed in 1 h ranged from 5000 μlL to 6000 μlL, i.e., a mass of sediment from 12.5 g to 15 g, when considering a sediment density of 2500 g L^{-1}. This mass settled in the area under study equalling 2.5 m of in length per

0.5 m in width. This results in a range in the sedimentation rate of 240–288 g m^{-2}·day^{-1}. This sedimentation rate within seagrass beds is greater than that found by some authors (Granata et al., 2001; Serra et al., 2020). However, sedimentation rates in seagrass beds varies through the year in the range of 1.5–500 g m^{-2}·day^{-1} (Gacia and Duarte, 2001). These sedimentation rate values align with those in the present study. However, note that high sedimentation rates might cause plant burial that can negatively affect the growth of plants, thus compromising their survival (Cabaço et al., 2008; Manzanera et al., 1998). Manzanera et al. (1998) found that an increase in sediment deposition producing a 15 cm change in sediment height produced total mortality of the seagrass after 200–300 days. In the present study, considering a volume of 5000 μL of sediment deposited after 1 h, it would require 37500 h (i.e., 10.4 days) to reach such a change (i.e.15 cm) in the height of the sediment.

Particle sedimentation onto the seabed was affected by the presence of canopies and had a greater impact on coarse, rather than fine, particles, between 5.7 - 10.9% and 11.0–14.4% higher in the presence of vegetation, respectively. The annual cycle of the seagrasses could imply different regimes of sedimentation due to the continuous loss and renewal of leaves. *Posidonia oceanica* leaves grow progressively from winter to summer, when they obtain their maximum extension (Gruber and Kemp, 2010). In contrast, from late summer to autumn they shed their leaves, causing an accumulation of leaf litter on the seabed until the energy flow is able to transport them away (Paladini de Mendoza et al., 2018). This indicates that, at the end of the plant cycle, a portion of the dead leaves is likely to ultimately be transported to the bottom. Therefore, this study states that the presence of the canopy enhances the flux of allochthonous particles down to the bed in two different ways: it increases the direct sedimentation to the bed (through a reduction in the *TKE*) and it captures particles on its blades that may eventually end up on the seabed when the blades die.

This study demonstrated that under oscillatory flow for both fine and coarse sediment particles, shoot density also increased the sediment deposited to the seabed and reduced the suspended sediment particles. This aligns with the results found by Wilkie et al. (2012), who claimed that under a unidirectional flow, sediment deposition increased with seagrass density.

4.5. Sediment balance between sediment trapped by plant blades and by the canopy

A partition coefficient higher than 18.5% for fine particles and 25.0% for coarse particles was found for low values of *TKE*, and which correspond to the highest canopy cover. This result indicates that a larger volume of suspended sediment was trapped on the surface of the plant leaves compared to the volume of suspended sediment that remained in suspension inside the canopy in denser canopies. This demonstrates the fact that, while denser canopies have fewer particles per blade, the higher density of the canopies balances this result, producing the greater overall particle trapping observed on blades in the denser canopies. These results show that, as has been pointed out by other authors (Hendriks et al., 2008; Short et al., 1984; Ackerman, 2002), a significant portion of the suspended particles transported inside the seagrass canopies collides with the leaves. For canopy covers over 52.1%, the trapping of fine particles on plant blades was greater than that for coarse particles, while with lower covers, the blades had the same ability to trap both fine and coarse particles. So, a threshold of $TKE = 0.36\ cm^2\ s^{-2}$ indicates that for *TKE* below this value, leaf blades are able to trap the different sized suspended sediment particles. In addition to canopy density, plant height might also impact the canopy cover because longer leaves can bend more and produce a greater cover under certain hydrodynamic conditions. This increase in the cover by larger plants can have an impact on the TKE. An increase in plant height has been found to increase wave attenuation (Pujol et al., 2013a; Koftis et al., 2011). Furthermore, during the leaf growth, leaves might shift from a more rigid to a more flexible structure which can also impact the canopy cover. Rigid canopy structures can reduce the energy of the flow by three times that of flexible canopies (Bouma et al., 2005). Therefore, more work should be done to assess the effect both plant height and flexibility have on the hydrodynamics and the ability to capture particles on the leaves.

4.6. Ecological implications

Through the flume laboratory experiments carried out in this study, results contribute to confirming those obtained in field surveys where the importance of preserving seagrass meadows has been clearly demonstrated. The laboratory results allow us to demonstrate that the presence of seagrass in coastal areas does in fact have direct ecological implications on marine ecosystems since it favours the preservation of marine coastal seabeds and, therefore, the accumulation of sediments that contribute to storing and preserving carbon from autochthonous and allochthonous sources within the context of climate change.

Seagrass canopies play a crucial role in determining the characteristics of the seabed. Van Katwijk et al. (van Katwijk et al., 2010) found, on the one hand, muddification (an increase in fine sediment on the seabed), in high density canopies and, on the other hand, sandification in sparse canopies which tended to have a greater concentration of large sized particles. These results agree with the increase in the ratio between the mass of fine to coarse particles attached to blades from sparse (with $\frac{V^F_{SP}}{V^C_{SP}} = 0.5\%$ for $SPF = 1\%$) to dense canopies ($\frac{V^F_{SP}}{V^C_{SP}} = 0.8\%$ for $SPF = 7.5\%$). A high level of attachment of fine particles to blades results from the increase in the available surface where particles can be deposited.

Brodersen et al. (2017a) found that the silt/clay sediment attached to leaves of *Zostera muelleri* Irmisch ex Ascherson, has negative effects on the activity and efficiency of photosynthesis and on the night-time O_2 exchange between the leaf tissue and the surrounding water. According to our study, seagrass meadows with high canopy cover values will reduce the sediment trapped by each plant, thus favouring photosynthetic activity and O_2 exchange, while the sediment trapped by the whole canopy will be greater, thus reducing turbidity. Therefore, the overall effect of dense canopies will be twofold, less suspended sediment and cleaner leaves, which result in water of a better quality with greater clarity that can fulfil the photosynthetic requirements of the vegetation. This result may explain the existence of a potential threshold for the status of the water quality due to the effect canopies have. From Lopez-y-Royo et al. (Lopez-y-Royo et al., 2011), the threshold for moderate to good status water quality in seagrasses was for a shoot density of 210 shoots m^{-2}. From the present study, such a shoot density corresponds to a canopy cover of 46.3%; which coincides with the threshold where the *Pc* became differential for fine and coarse particles, i.e., to the greater cover of 50%. Therefore, the fact that plant blades trap a smaller portion of coarse than fine particles, may be related to water quality. Since fine particles trapped by each plant remain constant, the effect on plant fitness is as a result of the coarse particles trapped by plants. We hypothesize that those lower values of coarse particles attached to the leaf blades of the plants will result in a thinner layer of sediment on the blades, thus allowing for a better gas exchange. Hence, photosynthetic activity is improved and so too the meadow's fitness. In addition, the reduction of suspended sediment within the canopy in the case of dense canopies, will improve the water quality of the ecosystem, producing positive feedback to the canopy.

Another important aspect of sediment deposition on seagrass meadows is the storage and preservation of carbon in the seabed which, by managing these ecosystems, would be a potential mechanism for mitigating CO_2 emissions. Ricart et al. (2015b) found a higher content of organic carbon inside the seagrass canopies than at the edges of the canopy. The results presented here substantiate the argument for the seagrass restoration programmes conducted world-wide since the mid-20th century to mitigate climate change (Paling et al., 2009), help

rebuild the lost carbon sink and conserve the remaining stores due to the ability of seagrass canopies to capture particles in an oscillatory flow.

5. Conclusions

Seagrasses impacted by allochthonous sediment sources decreased the amount of suspended sediment compared to unvegetated beds through two processes: the capture of sediment particles by plant blades, and the enhancement of particle sedimentation onto the seabed. The plant blades captured suspended particles settling through the water column. The denser the canopy was, the lower the percentage of particles trapped by the blades individually, but the greater the percentage trapped by the whole canopy. As a result, estimates of particle sedimentation onto the seabed increased with canopy cover, coinciding with a decrease in the *TKE*. Therefore, this study reports that an increase in canopy cover increases sedimentation and particle capture by the leaves of the plants and, therefore, impacts on the suspended sediment remaining in the water column inside the canopy in such a way that water clarity in dense seagrass canopies improves.

This study also reports that the sediment concentration obtained for coarse particles, either in suspension or trapped by the canopy, is greater than that for fine particles. The concentration of fine particles trapped by individual leaf blades, however, does not vary with canopy cover or with the *TKE*. In contrast, the concentration of coarse particles trapped by individual blades decreased as the canopy cover increased, i.e., as the *TKE* decreased. This means that for all the *TKE* ratios studied, plants were equally able to capture fine particles in suspension but not the coarse particle fractions, where a threshold for the *TKE* was observed. For canopy covers over 52%, the trapping of fine particles on the blades is greater than that for coarse particles. This canopy cover value represents a threshold for the maximum volume of particles blades in sparse canopies can capture, which might impact on their fitness.

To conclude, the presence of vegetation in seagrass beds increased the available surface on which particles can be deposited. In addition, the reduction of turbulence and flow velocities was enhanced by the presence of vegetation and increased with canopy density. Therefore, the overall trapping of particles by seagrasses, either through settling on the bed or being trapped by their leaves, produced a decrease in the suspended sediment concentration, enhancing the water quality and resulting in positive feedback for the seagrass itself.

CRediT authorship contribution statement

Aina Barcelona: Methodology, Investigation, Formal analysis, Data curation, Writing – original draft. **Carolyn Oldham:** Data curation, Writing – review & editing, Supervision. **Jordi Colomer:** Conceptualization, Methodology, Investigation, Data curation, Writing – review & editing. **Jordi Garcia-Orellana:** Conceptualization, Writing – review & editing. **Teresa Serra:** Conceptualization, Methodology, Investigation, Data curation, Writing – review & editing, Supervision.

Declaration of competing interest

The authors declare that they have no known competing financial interests or personal relationships that could have appeared to influence the work reported in this paper.

Acknowledgments

This research was funded by the University of Girona, through the grant MPCUdG2016-006 and by the Ministerio de Economía, Industria y Competitividad of the Spanish Government through the grant CGL2017-86515-P. This work contributes to the ICTA 'Unit of Excellence' (MinECo, MDM2015-0552) and the Generalitat de Catalunya research program (2017 SGR-1588). Aina Barcelona was funded by the pre-doctoral grant 2020 FI SDUR 00043 by the "Generalitat de Catalunya".

References

Ackerman, J.D., 2002. Diffusivity in a Marine macrophyte canopy: implications for submarine pollination and dispersal. Am. J. Bot. 89, 1119–1127.
Agawin, N.S.R., Duarte, C.M., 2002. Evidence of direct particle trapping by a tropical seagrass meadow. Estuaries 25, 1205–1209.
Armitage, A.R., Fourqurean, J.W., 2016. Carbon storage in seagrass soils: long-term nutrient history exceeds the effects of near-term nutrient enrichment. Biogeosciences 13, 313–321.
Bos, A.R., Bouma, T.J., de Kort, G.L.J., van Katwijk, M.M., 2007. Ecosystem engineering by annual intertidal seagrass beds: sediment accretion and modification. Estuar. Coast Shelf Sci. 74, 344–348.
Bouma, T.J., de Vries, M.B., Low, E., Peralta, G., T Nczos, I.C., van de Koppel, J., J Herman, P.M., 2005. Trade-off related to ecosystem engineering: a case study on stiffness of emerging macrophytes. Ecology 86 (8), 2187–2199.
Brodersen, K.E., Hammer, K.J., Schrameyer, V., Floytrup, A., Rasheed, M.A., Ralph, P.J., Kühl, M., Pedersen, O., 2017a. Sediment resuspension and deposition on seagrass leaves impedes internal plant aeration and promotes phytotoxic H_2S intrusion. Front. Plant Sci. 8, 1–13.
Brodersen, M.M., Panatzi, M., Kokkali, A., Panayotidis, P., Gerakaris, V., Maina, I., Kavadas, S., Kaber, H., Vassilopoulou, V., 2017b. Cumulative impacts from multiple human activities on seagrass meadow in eastern Mediterranean waters: the case of Saronikos Gulf (Aegean Sea, Greece). Environ. Sci. Pollut. Res. 25, 26809–29822.
Cabaço, S., Santos, R., Duarte, C.M., 2008. The impact of sediment burial and erosion on seagrasses: a review. Estuar. Coast Shelf Sci. 79, 354–366.
Colomer, J., Boubnov, B.M., Fernando, H.J.S., 1999. Turbulent convection from isolated sources. Dynam. Atmos. Oceans 30, 125–148.
Colomer, J., Soler, M., Serra, T., Casamitjana, X., Oldham, C., 2017. Impact of anthropogenically created canopy gaps on wave attenuation in a *Posidonia oceanica* seagrass meadow. Mar. Ecol. Prog. Ser. 569, 103–116.
Community, European, 2000. Directive 2000/60/EC of the European Parliament and of the Council of 23 October 2000 establishing a framework for Community action in the field of water policy. Off J Eur Communities L327.
Duarte, C.M., 1991. Seagrass depth limits. Aquat. Bot. 40 (4), 363–377.
Duarte, C.M., Sintes, T., Marbà, N., 2013. Assessing the CO_2 capture potential of seagrass restoration projects. J. Appl. Ecol. 50, 1341–1349.
Duarte, C.M., Borja, A., Carstensen, J., Elliott, M., Krause-Jensen, D., Marbà, N., 2015. Paradigms in the recovery of estuarine and coastal ecosystems. Estuar. Coast 38, 1202–1212.
Folkard, A., 2005. Hydrodynamics of model *Posidonia oceanica* patches in shallow water. Limnol. Oceanogr. 50, 1592–1600.
Fourqurean, J.W., Duarte, C.M., Kennedy, H., Marbà, N., Holmer, M., Mateo, M.A., Apostolaki, E.T., Kendrick, G.A., Krause-Jensen, D., McGathery, K.J., Serrano, O., 2012. Seagrass ecosystems as a globally significant carbon stock. Nat. Geosci. 5, 505–509.
Fraser, M.W., Short, J., Kendrick, G., McLean, D., Keesing, J., Byrne, M., Caley, M.J., Clarke, D., Davis, A.R., Erftemeijer, P.L.A., Field, S., Gustin-Craig, S., Huisman, J., Keough, M., Lavery, P.S., Masini, R., McMahon, K., Mengersen, K., Rasheed, M., Statton, J., Stoddart, J., Wu, P., 2017. Effects of dredging on critical ecological processes for marine invertebrates, seagrasses and macroalgae, and the potential for management with environmental windows using Western Australia as a case study. Ecol. Indicat. 78, 229–242.
Gacia, E., Duarte, C.M., 2001. Sediment retention by a Mediterranean *Posidonia oceanica* meadow: the balance between deposition and resuspension. Estuar. Coast Shelf Sci. 52, 505–514.
Gacia, E., Granata, T.C., Duarte, C.M., 1999. An approach to measurement of particle flux and sediment retention within seagrass (*Posidonia oceanica*) meadows. Aquat. Bot. 65, 255–268.
Ghisalberti, M., Nepf, H., 2002. Mixing layers and coherent structures in vegetated aquatic flows. J. Geophys. Res. 107, C23011.
González-Ortiz, V., Egea, L.G., Jiménez-Ramos, R., Moreno-Marín, F., Pérez-Lloréns, J.L., Bouma, T., Brun, F., 2016. Submerged vegetation complexity modifies benthic infauna communities: the hidden role of the belowground system. Mar. Ecol. 37, 543–552.
Goring, D.G., Nikora, V.I., 2002. Despiking acoustic Doppler velocimeter data. J. Hydraul. Eng. 128, 117–126.
Grabowski, R.C., Droppo, I.G., Wharton, G., 2011. Erodibility of cohesive sediment: the importance of sediment properties. Earth Sci. Rev. 105 (3–4), 101–120.
Granata, T.C., Serra, T., Colomer, J., Casamitjana, X., Duarte, C.M., Gacia, E., 2001. Flow and particle distributions in a nearshore seagrass meadow before and after a storm. Mar. Ecol. Prog. Ser. 218, 95–106.
Greiner, J.T., Wilkinson, G.M., McGlathery, K.J., Emery, K.A., 2016. Sources of sediment carbon sequestered in restored seagrass meadows. Mar. Ecol. Prog. Ser. 551, 95–105.
Gruber, R.K., Kemp, W.M., 2010. Feedback effects in a coastal canopy-forming submersed plant bed. Limnol. Oceanogr. 55, 2285–2298.
Hendriks, I.E., Sintes, T., Bouma, T.J., Duarte, C.M., 2008. Experimental assessment and modeling evaluation of the seagrass *Posidonia oceanica* on flow and particle trapping. Mar. Ecol. Prog. Ser. 356, 163–173.
Hendriks, I.E., Bouma, T.J., Morris, E.P., Duarte, C.M., 2010. Effects of seagrass and algae of the *Caulerpa* family on hydrodynamics and particle-trapping rates. Mar. Biol. 157, 473–481.
Howe, A.J., Rodríguez, J.F., Saco, P.M., 2009. Surface evolution and carbon sequestration in disturbed and undisturbed wetland soils of the Hunter estuary, southeast Australia. Estuar. Coast Shelf Sci. 84, 75–83.

Howley, C., Devlin, M., Burford, M., 2018. Assessment of water quality from the Normanby River catchment to coastal flood plumes on the northern Great Barrier Reef, Australia. Mar. Freshw. Res. 69 (6), 859–873.
Iafrati, A., 2011. Energy dissipation mechanisms in wave breaking process: spilling and highly aerated plunging breaking events. J. Geophys. Res. 16, C07024.
Islam, M., Jahra, F., Hiscock, S., 2016. Data analysis methodologies for hydrodynamic experiments in waves. J. Nav. Architect. Mar. Eng. 13 (1), 1–15.
Koftis, T., Prinos, P., January, (, 2011. Estimation of wave attenuation over *Posidonia oceanica*. In: 5th International Short Conference on Applied Coastal Research. Aachen, Germany.
Lawson, S.E., McGlathery, K.J., Wilberg, P.L., 2012. Enhancement of sediment suspension and nutrient flux by benthic macrophytes at low biomass. Mar. Ecol. Prog. Ser. 448, 259–270.
Le Méhauté, B., 1976. An Introduction to Hydrodynamics & Water Waves, first ed. (California: Pasadena).
Longstaff, B.J., Dennison, W.C., 1999. Seagrass survival during pulsed turbidity events: the effects of light deprivation on the seagrasses *Halodule pinifolia* and *Halophila ovalis*. Aquat. Bot. 65, 105–121.
Lopez-y-Royo, C., Pergent, G., Alcoverro, T., Buia, M.C., Casazza, G., Martínez-Crego, B., Pérez, M., Silvestre, F., Romero, J., 2011. The seagrass *Posidonia oceanica* as indicator of coastal water quality: experimental intercalibration of classification systems. Ecol. Indicat. 11, 557–563.
Lovelock, C.E., Adame, M.F., Bennion, V., Hayes, M., O'Mara, J., Reef, R., Santini, N.S., 2014. Contemporary rates of carbon sequestration through vertical accretion of sediments in mangrove forest and saltmarshes of South East Queensland, Australia. Estuar. Coast 37, 763–771.
Lowe, R.J., Koseff, J.R., Monismith, S.G., 2005. Oscillatory flow through submerged canopies: 2. Canopy mass transfer. J. Geophys. Res. 110, C10017.
Luhar, M., Coutu, S., Infantes, E., Fox, S., Nepf, H., 2010. Wave-induced velocities inside a model seagrass bed. J. Geophys. Res. 115, C12005.
Manzanera, M., Pérez, M., Romero, J., 1998. Seagrass mortality due to over sedimentation: an experimental approach. J. Coast Conserv. 4 (1), 67–70.
Marbà, N., Arias-Ortiz, A., Masqué, P., Kendrick, G.A., Mazarrassa, I., Bastyan, G.R., Garcia-Orellana, J., Duarte, C.M., 2015. Impact on seagrass loss and subsequent revegetation on carbon sequestration and stocks. J. Ecol. 103, 296–302.
Mulder, T., Syvitski, J.P.M., 1995. Turbidity currents generated at river mouths during exceptional discharges to the world oceans. J. Geol. 103, 285–299.
Oey, L., L Mellor, G., 1993. Subtidal variability of estuarine outflow, plume, and coastal current: a model study. J. Phys. Oceanogr. 23, 164–171.
Paladini de Mendoza, F., Fontolan, G., Mancini, E., Scanu, E., Scanu, S., Bonamano, S., Marcelli, M., 2018. Sediment dynamics and resuspension processes in a shallow-water *Posidonia oceanica* meadow. Mar. Geol. 404, 174–186.
Paling, E.I., Fonseca, M., van Katwijk, M.M., van Keulen, M., 2009. Seagrass restoration. In: Perillo, G., Wolanski, E., Cahoon, D., Brinson, M. (Eds.), Coastal Wetlands: an Integrated Ecosystems Approach. Elsevier, Amsterdam, pp. pp687–713.
Palmer, M.R., Nepf, H., Ackerman, J.D., 2004. Observations of particle capture on a cylindrical collector: implications for particle accumulation and removal in aquatic systems. Limnol. Oceanogr. 49, 76–85.
Pascolo, S., Petti, M., Bosa, S., 2019. Wave forecasting in shallow water: a new set of growth curves depending on bed roughness. Water 11, 2313.
Pineda, M.-C., Strehlow, B., Kamp, J., Duckworth, A., Jones, R., Webster, N.S., 2016. Effects of combined dredging-related stressors on sponges: a laboratory approach using realistic scenarios. Sci. Rep. 7, 5155.
Pujol, D., Nepf, H., 2012. Breaker-generated turbulence in and above a seagrass meadow. Continent. Shelf Res. 49, 1–9.
Pujol, D., Colomer, J., Serra, T., Casamitjana, X., 2010. Effect of submerged aquatic vegetation on turbulence induced by an oscillatory grid. Continent. Shelf Res. 30, 1019–1029.
Pujol, D., Casamitjana, X., Serra, T., Colomer, J., 2013a. Canopy-scale turbulence under oscillatory flow. Continent. Shelf Res. 66, 9–18.
Pujol, D., Serra, T., Colomer, J., Casamitjana, X., 2013b. Flow structure in canopy models dominated by progressive waves. J. Hydrol. 486, 281–292.
Ricart, A.M., York, P.H., Rasheed, M.A., Pérez, M., Romero, J., Bryant, C.V., Macreadie, P.I., 2015. Variability of sedimentary organic carbon in patchy seagrass landscapes. Mar. Pollut. Bull. 100, 476–482.
Ricart, A.M., Pérez, M., Romero, J., 2017. Landscape configuration modulates carbon storage in seagrass sediments. Estuar. Coast Shelf Sci. 185, 69–76.
Ros, À., Colomer, J., Serra, T., Pujol, D., Soler, M., Casamitjana, X., 2014. Experimental observations on sediment resuspension within submerged model canopies under oscillatory flow. Continent. Shelf Res. 91, 220–231.
Roy, E.D., White, J.R., Smith, E.A., Bargu, S., Li, C., 2013. Estuarine ecosystem response to three large-scale Mississippi River flood diversion events. Sci. Total Environ. 458, 374–387.
Serra, T., Colomer, J., Cristina, X., Vila, X., Arellano, J.B., Casamitjana, X., 2001. Evaluation of a laser in situ scattering instrument for measuring the concentration of phytoplankton, purple sulphur bacteria and suspended inorganic sediments in lakes. J. Environ. Eng. 127, 1023–1030.
Serra, T., Colomer, J., Gacia, E., Soler, M., Casamitjana, X., 2002a. Effects of a turbid hydrothermal plume on the sedimentation rates in a karstic lake. Geophys. Res. Lett. 29, 1–5.
Serra, T., Colomer, J., Zamora, L., Moreno-Amich, R., Casamitjana, X., 2002b. Seasonal development of a turbid hydrothermal lake plume and the effects on the fish distribution. Water Res. 36, 2753–2760.
Serra, T., Oldham, C., Colomer, J., 2018. Local hydrodynamics at edges of marine canopies under oscillatory flows. PloS One 13, e0201737.
Serra, T., Gracias, N., Hendriks, I., 2020. Fragmentation in seagrass canopies can alter hydrodynamics and sediment deposition rates. Water 12 (12), 3473.
Short, F.T., Short, C.A., 1984. The seagrass filter: purification of estuarine and coastal waters. In: Kennedy, V.S. (Ed.), The Estuary as a Filter, pp. pp395–413.
Smith, M.J., Stevens, C.L., Gorman, R.A., McGregor, J.A., Neilson, C.G., 2001. Wind-wave development across a large shallow intertidal estuary: a case study of Manukau Harbour, New Zealand. N.Z.J. Mar. Freshwater. Res. NEW ZEAL J MAR FRESH. 35 (5), 985–1000.
Sridhar, P.N., Ramana, I.V., Jaya Kumar, S., 2014. Seasonal occurrence of unique sediment plume in the Bay of Bengal. Eos Transactions American Geophysical Union 89 (3), 22–23.
Terrados, J., Duarte, C.M., 2000. Experimental evidence of reduced particle resuspension within a seagrass (*Posidonia oceanica* L.) meadow. J. Exp. Mar. Biol. Ecol. 243, 45–53.
van Katwijk, M.M., Bos, A.R., Hermus, D.C.R., Suykerbuyk, W., 2010. Ediment modification by seagrass beds: muddification and sandification induced by plant cover and environmental conditions. Estuar. Coast Shelf Sci. 89, 175–181.
Vanderploeg, H.A., Johenger, T.H., Lavrentyev, P.J., Chen, C., Lang, G.A., Agy, M.A., Bundy, M.H., Cavaletto, J.F., Eadie, B.J., Liebig, J.R., Miller, G.S., Ruberg, S.A., McCormick, M.J., 2007. Anatomy of the recurrent coastal sediment plume in Lake Michigan and its impacts on light climate, nutrients, and plankton. J. Geophys. Res. 112, C03S90.
Vautard, R., Bobiet, A., Sobolowski, S., Kjellström, E., Stegehuis, A., Watkiss, P., Mendlik, T., Landgren, O., Nikulin, G., Teichmann, C., Jacob, D., 2014. The European climate under a 2°C global warming. Environ. Res. Lett. 9, 034006.
Wilkie, L., O'Hare, M.T., Davidson, I., Dudley, B., Paterson, D.M., 2012. Particle trapping and retention by *Zostera noltii*: a flume and field study. Aquat. Bot. 102, 15–22.
Wu, P.P.-Y., McMahon, K., Rasheed, M.A., Kendrick, G.A., York, P.H., Chartrand, K., Caley, M.J., Mengersen, K., 2017. Managing seagrass resilience under cumulative dredging affecting light: predicting risk using dynamic Bayesian networks. J. Appl. Ecol. 55, 1339–1350.
Zhang, X., Nepf, H., 2008. Density-driven exchange flow between on water and an aquatic canopy, Water. Resour. Res. 44, W08417.
Zhang, Y., Nepf, H., 2019. Wave-driven sediment resuspension within a model eelgrass meadow. J. Geophys. Res.-Earth 124, 1035–1053.
Zhang, Y., Tang, C., Nepf, H., 2018. Turbulent kinetic energy in submerged model canopies under oscillatory flow, Water. Resour. Res. 54, 1734–1750.
Zong, L., Nepf, H., 2011. Spatial distribution of deposition within a patch of vegetation. Water Resour. Res. 47, W03516.
Zucchetta, M., Veiner, C., Taji, M.A., Mangin, A., Pastres, R., 2016. Modelling the spatial distribution of the seagrass *Posidonia oceanica* along the north african coast: implications for the assessment of good environmental status. Ecol. Indicat. 61, 1011–1023.